Available online at www.sciencedirect.com

SCIENCE DIRECT®

Tectonophysics 388 (2004) 173–185

TECTONOPHYSICS

www.elsevier.com/locate/tecto

Seismic studies of the Brasília fold belt at the western border of the São Francisco Craton, Central Brazil, using receiver function, surface-wave dispersion and teleseismic tomography

Marcelo Assumpção*, Meijian An, Marcelo Bianchi, George S.L. França, Marcelo Rocha, José Roberto Barbosa, Jesús Berrocal

Institute of Astronomy, Geophysics and Atmospheric Sciences, University of São Paulo, Rua do Matão 1226, São Paulo, SP, 05508-090 Brazil

Received 25 July 2003; received in revised form 19 April 2004; accepted 13 June 2004
Available online 25 August 2004

Abstract

The Tocantins Province in Central Brazil is composed of a series of SSW–NNE trending terranes of mainly Proterozoic ages, which stabilized in the Neoproterozoic in the final collision between the Amazon and São Francisco cratons. No previous information on crustal seismic properties was available for this region. Several broadband stations were used to study the regional patterns of crustal and upper mantle structure, extending the results of a recent E–W seismic refraction profile. Receiver functions and surface wave dispersion showed a thin crust (33–37 km) in the Neoproterozoic Magmatic Arc terrane. High average crustal Vp/Vs ratios (1.74–1.76) were consistently observed in this unit. The foreland domain of the Brasília foldbelt, on the other hand, is characterized by thicker crust (42–43 km). Low Vp/Vs ratios (1.70–1.72) were observed in the low-grade foreland fold and thrust zone of the Brasília belt adjacent to the São Francisco craton. Teleseismic P-wave tomography shows that the lithospheric upper mantle has lower velocities beneath the Magmatic Arc and Goiás Massif compared with the foreland zone of the belt and São Francisco craton. The variations in crustal thickness and upper mantle velocities observed with the broadband stations correlate well with the measurements along the seismic refraction profile. The integration of all seismic observations and gravity data indicates a strong lithospheric contrast between the Goiás Massif and the foreland domain of the Brasília belt, whereas little variation was found across the foldbelt/craton surface boundary. These results support the hypothesis that the Brasília foreland domain and the São Francisco craton were part of a larger São Francisco-Congo continental plate in the final collision with the Amazon plate.

Keywords: Receiver function; Poisson's ratio; Tomography; Lithosphere; São Francisco craton; South America

* Corresponding author.
E-mail address: marcelo@iag.usp.br (M. Assumpção).

0040-1951/$ - see front matter © 2004 Elsevier B.V. All rights reserved.
doi:10.1016/j.tecto.2004.04.029

1. Introduction

The Tocantins Province in central Brazil (Fig. 1) is a Neoproterozoic orogen resulting from the collisional history between two major cratons in South America: the Amazon and the São Francisco cratons (e.g., Pimentel and Fuck, 1992; Pimentel et al., 1999). Little is known about the deep crustal structure of this area as no previous investigation of the crustal seismic structure had been carried out in central Brazil before the recent seismic refraction line of Berrocal et al. (2004, this issue) shown in Fig. 1b. A steep Bouguer gravity gradient surrounds the São Francisco craton all along its southwestern and western border (Fig. 1a), with high gravity values to the west (Bouguer anomalies up to +30 mGal) and low values to the east (down to −140 m Gal) where a possible continental margin is buried by metasediments. How much of this gravity difference is caused by variations of crustal thickness or mean crustal density is not known. Also, the western boundary of the São Francisco craton is gradational with low grade metasediments of the external zone changing into high grade metamorphic complexes of the internal zone (Fig. 1b), making the exact boundary of the craton at depth a matter of dispute (Alkmin et al., 1993).

To address these questions, a seismic refraction line was recently shot along an E–W transect in the central part of the Tocantins province (Fig. 1b). The seismic refraction data (Berrocal et al., 2004) showed that the Magmatic Arc and the Goiás Massif have thinner crust (33–36 km) and upper mantle velocities of 8.0 km/s. The external, foreland zone of the Brasilia belt has a thicker crust (40–43 km) and a higher Pn velocity of 8.2 km/s. Average crustal P-wave velocities are slightly higher beneath the Magmatic Arc (6.4 km/s) compared with the foreland zone of the Brasília belt (6.3 km/s). Studies of receiver function and surface wave dispersion were carried out with broadband stations installed in the central and southern part of the province, extending the results of the seismic refraction line located further north (Fig. 1b). The five temporary

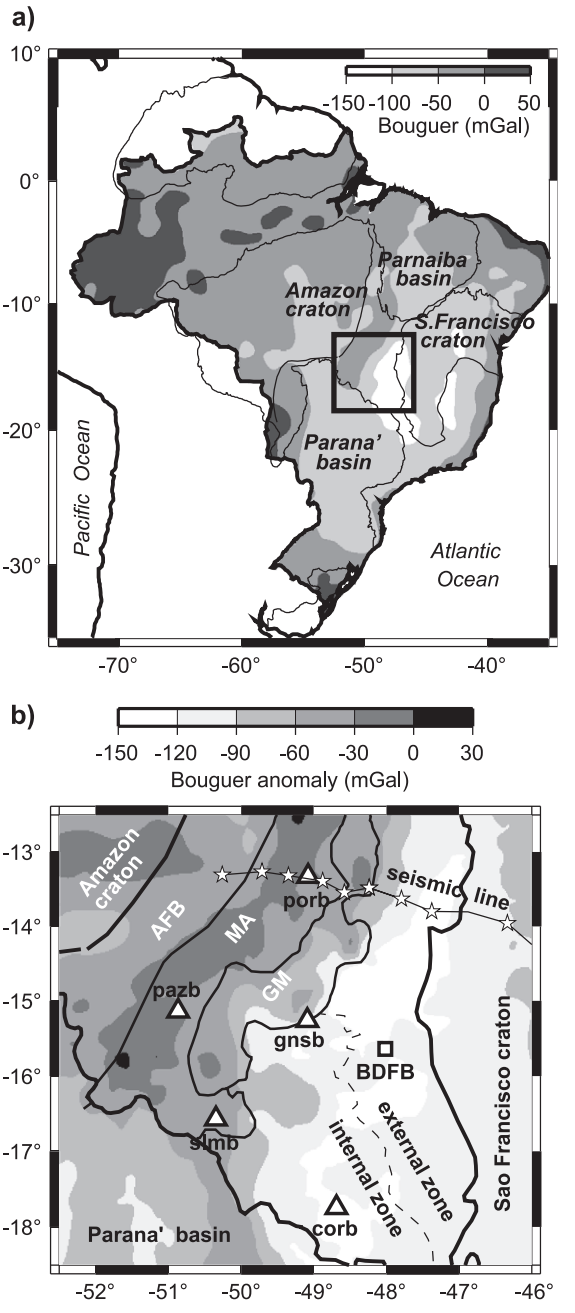

Fig. 1. (a) Location of the study area in the Tocantins Province (rectangle) with the regional Bouguer gravity anomalies (Sá et al., 1993) and the main geological provinces in Brazil. (b) Study area with the broadband seismic stations (triangles are temporary stations; square is a permanent station) and the seismic refraction line with shots denoted by stars. The main geological units (Pimentel et al., 2000) are: AFB=Araguaia fold belt, MA=Magmatic Arc, GM=Goiás Massif. The dashed line separates the internal zone (high grade metamorphic complexes), from the external zone with low grade metasediments of the foreland domain of the fold-and-thrust belt. Gray shades are Bouguer gravity from Marangoni et al. (1995).

stations operated for 2 years, on average. Together with the Brasília permanent station (BDFB), they allow estimates of crustal thickness and average Vp/Vs ratios. Here, we present the analyses of receiver functions, a study of surface wave dispersion for the path PAZB-PORB along the Magmatic Arc unit, and integrate these results with those of teleseismic P-wave tomography.

The northern part of the Tocantins Province consists of a Neoproterozoic orogen and is underlain mainly by the Araguaia fold-and-thrust belt (flanking the eastern margin of the Amazon craton) and by the Brasília Belt at the western margin of the São Francisco Craton. The main geological units in the Brasília Belt domain are (Fig. 1b): (1) a SSW–NNE trending Neoproterozoic Magmatic Arc terrane, formed as an island arc system off the coast of the São Francisco-Congo continent, which started operating around 890 Ma with final ocean closure and continent collision at ca. 600 Ma (Pimentel and Fuck, 1992; Pimentel et al., 1991, 1997; Junges et al., 2002); (2) the Goiás Massif, an assembly of gneissic-granitic rocks of various ages, mainly Paleoproterozoic, including Archean granite-greenstone terrains in the central part (Pimentel et al., 2000); (3) an "internal zone" with high-grade metamorphic complexes (Piuzana et al., 2003); and (4) an "external zone" with low grade metasediments of Neoproterozoic passive margin sequences. The Magmatic Arc and the Goiás Massif are characterized by high Bouguer gravity anomalies (Fig. 1b) and lower topography. In contrast, the foreland domain of the Brasília belt is characterized by low Bouguer anomalies and higher altitudes.

2. Crustal thicknesses and Vp/Vs ratios from receiver functions

Large earthquakes (m_b>~5.7) mostly in the distance range 25–88° were used for the receiver function analysis. Most events came from SW, W and NW back-azimuths due to the larger seismicity of the Andean and Central America regions, but we also used events from other azimuths whenever possible. We used the frequency domain deconvolution technique (Owens et al., 1984; Ammon et al., 1990) with a low-pass gaussian filter [$\exp(-(\omega^2/4\alpha^2)$] with parameter α=2 or 4 s^{-1}, corresponding to a corner frequency of about 1 or 2 Hz. A specific time window, in the range 40 s–90 s, was chosen for each event to produce the best receiver function with the least instabilities and lowest amplitudes before the arrival of the "direct" P-wave.

Although modeling the whole receiver function waveform can yield a detailed velocity-depth profile, the inversion is highly non-unique (e.g., Ammon et al., 1990). Also, scattered energy from lateral faults or discontinuities can significantly perturb the radial receiver functions (e.g., Abers, 1998), so the assumption of horizontal plane layers is usually questionable for detailed 1D inversion. For this reason, we only use the arrival times of the Moho converted phases, which are the most robust information contained in the receiver function, to estimate the crustal thickness and the average Vp/Vs ratio.

Fig. 2 shows the nine best receiver functions for station PAZB where the Moho converted Ps phase is easily identified at about 4-s delay time. The multiply reflected phases, however, are much more difficult to identify. Both the PpPms phase (a P-wave reflected at the surface and converted to S upon its

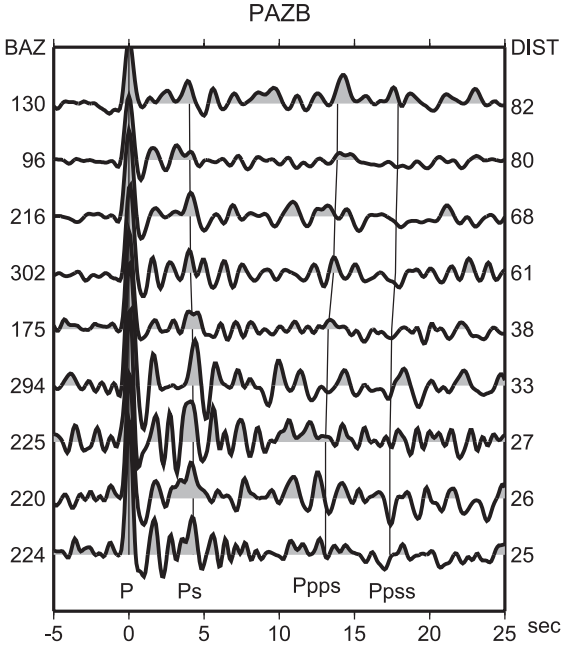

Fig. 2. Receiver functions for station PAZB. Backazimuths ("BAZ") and epicentral distances ("DIST"), in degrees, are indicated on each side of the plot. The vertical lines indicate the times for the phases Ps, Ppps and Ppss, expected for the crustal thickness and Vp/Vs ratio of Table 1.

reflection at the Moho, called here "Ppps", for simplicity) and the PpSmS+PsPms phase (called here "Ppss") can be used to determine the average crustal Vp/Vs ratio. Uncertainties in the Vp/Vs ratio have a larger effect on estimates of crustal thickness compared to uncertainties in the average P-wave velocity (Zandt and Ammon, 1995; Zandt et al., 1995). For this reason, processing techniques to enhance the multiple phases are essential for more accurate estimates of crustal thicknesses. One common technique (Zhu and Kanamori, 2000) is to search for the best crustal thickness and Vp/Vs ratio by maximizing the sum of the amplitudes of the three main phases at the times expected for a one-layer model.

Here, we used a different technique trying to enhance each of the three phases separately. The time difference Ps-P decreases with epicentral distance, whereas the time differences Ppps-P and Ppss-P increase with distance (Figs. 2 and 3.) This move-out varies with epicentral distance in a non-linear way (Fig. 3). For this reason, we used a new slant stacking technique whereby the epicentral distance is replaced by the square of the slowness. This variable substitution linearizes the move-out of the converted phases making it possible to slant stack all receiver functions without the need of an assumed velocity model. For each stacking inclination (slope), the stacked trace is also weighted by the average phase of the analytical signals of the individual traces to enhance coherent phases and reduce high amplitude, non-coherent noise (Schimmel and Paulssen, 1997). With this slant stacking technique, the slope helps identify the multiple Ppps and Ppss phases, as used successfully by França and Assumpção (2004).

Fig. 4 shows a contour diagram of the stacked amplitude for slopes varying from −0.035 to 0.025 $s/(s/^\circ)^2$. Positive and negative amplitudes are contoured with solid and dashed gray lines, respectively. The solid black lines show 90% of the amplitude of each peak and indicate the observed phases (Ps at 4.10 s, Ppps at 13.20 s and Ppss at 17.36 s). Note that the Ppps phase is positive, whereas the Ppss phase has negative amplitude. The observed times of each phase are then used to calculate the best Vp/Vs ratio and crustal thickness by least-squares. The triangles indicate the expected peaks for the best Vp/Vs (1.763) and crustal thickness (33.23 km), with the expected slopes taken from plots like Fig. 3. The advantage of this method is that each phase can be identified not only by its arrival time but also by its characteristic

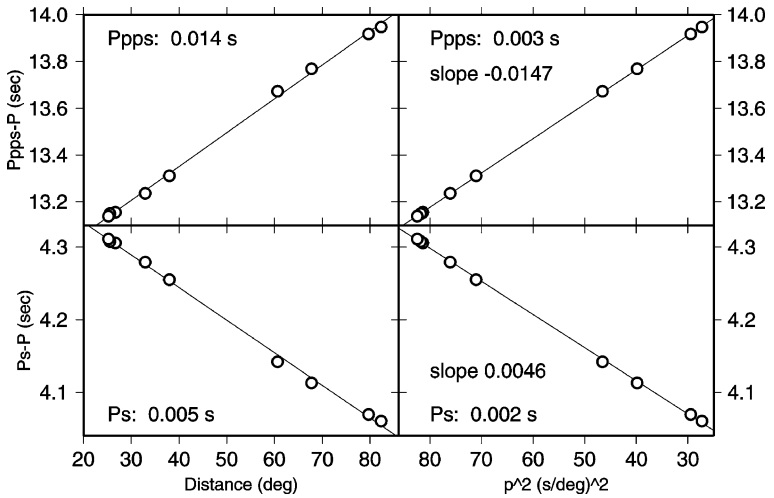

Fig. 3. Theoretical delay times for the Ps (bottom plots) and Ppps (upper plots) phases for the one-layer crustal model of station PAZB (Table 1). The nine data points were chosen according to the distances of the receiver functions (Fig. 2). The left plots show the variation of the delay times with epicentral distance; the right plots show the variation with the square of the slowness. The numbers beside the phase identification are the rms residual for a straight line fit. Note that the delay times are more linearly related to the square of the slowness. The calculated slopes are used to plot the triangles in Fig. 4.

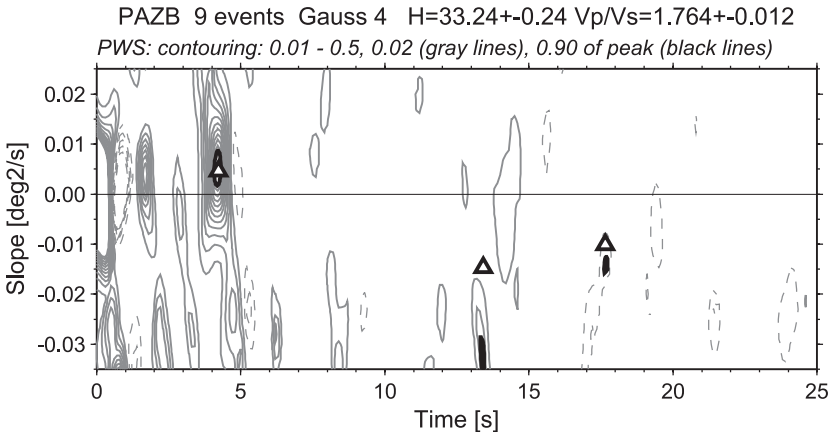

Fig. 4. Contour diagram of the slant-stacked amplitudes of the nine receiver functions from Fig. 2. The horizontal scale is the time from the direct P arrival for a reference slowness of 8.0 s/°; the vertical scale is the slope used for the slant-stacking. The large clipped peak at (0,0) is the direct P wave. Gray solid lines are positive amplitudes, gray dashed lines are negative amplitudes. The thick solid lines indicate 90% of the amplitude of each peak: Ps at 4.10 s, Ppps at 13.30 s and Ppss at 17.36 s. The triangles indicate the expected times and slopes for the one-layer model of Table 1.

move-out, independently of the assumed crustal velocity; the consistency among the three arrival times gives more confidence to the calculated Vp/Vs ratio.

Station PAZB, shown in Figs. 2 and 4, is an average quality temporary station. Fig. 5 shows the results for BDFB, a better, lower noise permanent station. For the record section in Fig. 5a, we used 52 earthquakes, some of them stacked in narrow bins of distance and azimuth. The phase-weighted slant-stacked contours (Fig. 5b) show the three converted phases very clearly as single peaks near the expected time and slope.

Table 1 shows the results of our method for all analysed stations, together with the estimated values from the grid-search method of Zhu and Kanamori (2000). The two methods agree as expected. The calculation of Vp/Vs ratio requires the average crustal Vp to be known, which was taken from the seismic profile in the northern part of the Tocantins Province (Berrocal et al., 2004). Station PORB lies on this seismic line (Fig. 1b) and the crustal depth given by the receiver function (37±1 km) is very close to the depths obtained from the seismic refraction line which vary from 34 to 36 km near the station.

Fig. 6 shows a record section of the stacked receiver functions, after correction for the move-out of the Ps and the Ppps phases. The Ps phase is clear and sharp in all stations, as seen in the top part of Fig. 6 from 0 to 10 s . The traces from 10 to 25 s were stacked to enhance the reflected Ppps phase. With the exception of station CORB, the Ppps phase is clearly recognized as an isolated positive peak shown by the dashed line. If the crust were made of horizontal plane layers, the time difference Ppss-Ppps would be the same as the Ps-P time. In Fig. 6, the dashed line “Ppss” was drawn after the picked Ppps phase using the Ps-P difference. It can be seen that the multiple S reflection Ppss (which has negative amplitude) is consistently observed in most stations, despite the stacking slope not being the most appropriate to enhance it. The three stations in the Brasília belt show consistently longer Ps and Ppps times, indicating thicker crust, compared with the Magmatic Arc.

Thinner crust is observed for the stations on the Magmatic Arc (33–37 km) where altitudes are generally low and Bouguer anomalies are high (Fig. 6, bottom part). The stations in the foreland zone of the belt tend to have thicker crust (42–43 km). Station GNSB lies at the eastern boundary of the Goiás Massif defined by a shallow NW dipping thrust fault, so its receiver function is actually sampling the crust of the foreland domain. This pattern of crustal thickness and gravity data is consistent with isostatic compensation being achieved primarily by crustal thickness variations.

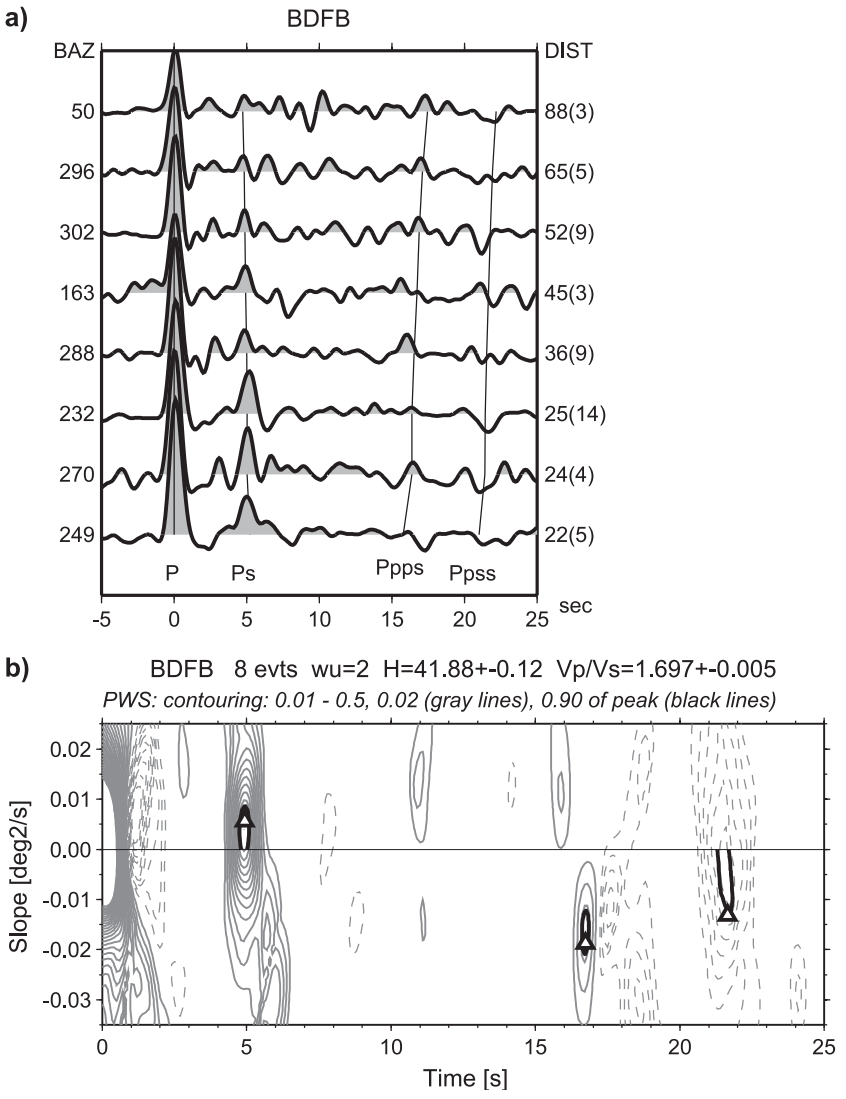

Fig. 5. (a) Receiver functions for the permanent station BDFB. Backazimuths and epicentral distances (in degrees) are indicated on each side of the plot. Each trace is actually a stack of several events with similar distances and azimuth; number of events for each stack is in parenthesis beside the distance. The vertical lines indicate the times for the phases Ps, Ppps and Ppss, expected for the crustal thickness and Vp/Vs ratio of Table 1. (b) Contour diagram of the slant-stacked amplitudes of the eight traces from (a). Note the clear peaks for all converted phases: Ps at 4.92 s, Ppps at 16.72 s and Ppss at 21.68 s. The triangles are the fitted data from the Vp/Vs and crustal thickness shown in Table 1.

Another interesting observation is that Vp/Vs ratios are higher (1.74–1.76) in the Magmatic Arc compared with the foreland domain (1.70–1.72). Holbrook et al. (1992) and Christensen (1996) showed that most lower crustal rocks with high Vp/Vs ratios tend to be mafic granulites. It is well known that higher silica content decreases Vp/Vs ratio (e.g., Christensen, 1996). Our Vp/Vs results may indicate a more felsic lower crustal composition for the external zone of the Brasília belt, compared with the Magmatic Arc.

The results for the southernmost station CORB, within a high grade metamorphic complex of the foreland belt, are not well constrained because of the difficulty in identifying the multiple reflections Ppps and Pssp. For this reason we refrain from

Table 1
Vp/Vs ratios and crustal thicknesses from receiver function analysis

Station	Altitude (m)	N	Distance range (°)	$(Ps–P)_0$ (s)	V_p (km/s)	Vp/Vs (pwss)	Vp/Vs (g-s)	Crustal thickness (km)	
								pwss	g-s
PAZB	410	9	25–82	3.92±0.05	6.41	1.76±0.01	1.77	33.2±0.4	32.8
PORB	365	6	29–78	4.29±0.03	6.41	1.75±0.02	1.73	37.1±0.9	37.5
SLMB	700	10	25–89	3.94±0.10	6.37	1.74±0.01	1.73	33.0±0.7	33.5
GNSB	1100	14	19–78	4.79±0.05	6.37	1.72±0.01	1.69	42.6±0.9	43.1
BDFB	1095	52	22–88	4.61±0.06	6.32	1.70±0.01	1.70	41.9±0.8	42.0
CORB	950	11	25–64	4.98±0.05	6.32	1.81 ?	1.85 ?	39 ?	38 ?

N=number of earthquakes used in the receiver function analysis; $(Ps-P)_0$=Ps-P time difference extrapolated for vertical incidence; uncertainties from bootstrap tests; V_p=average crustal P velocity (Berrocal et al., 2004) used to convert Ps-P to crustal thickness; Vp/Vs: pwss=phase-weighted slant-stack technique; g-s=grid-search method (Zhu and Kanamori, 2000); uncertainties in Vp/Vs and crustal thickness estimated by adding the variance from the pwss technique and the variance caused by an uncertainty of ±0.1 km/s in V_p.

interpreting the possibly high Vp/Vs ratio (1.81?–1.85?). Note, however, that the Ps phase is very clear (Fig. 6) and if a standard Vp/Vs ratio of 1.73 were used, the crustal thickness would be about 45 km, the thickest in our study area, consistent with the low Bouguer anomaly and high altitude.

3. Surface wave dispersion

Interstation Rayleigh and Love wave phase velocities were determined for the path PORB-PAZB, along the Magmatic Arc terrane. Teleseismic events were selected with propagation path no more than 5° off the great-circle between the two stations, as shown in Table 2. This criterion restricted our dataset to only four events of good quality.

Preliminary surface-wave group velocities were determined by multi-filtering technique (e.g., Herrmann, 1973). These initial velocities were used to isolate the fundamental mode using phase-matched filter (Herrin and Goforth, 1977; Herrmann, 1987) to remove interfering, scattered body waves and higher-mode surface waves. The isolated traces were cross correlated to calculate the phase velocity between the two stations (Herrmann, 1987). Fig. 7 shows the observed inter-station phase velocities.

3.1. Inversion and results

An inversion by Genetic Algorithm was carried out using horizontal homogeneous plane layers. The search parameters were both the S wave velocity (Vs) and thickness of each layer. The models had a fixed Vp/Vs ratio of 1.75, the average value beneath PAZB and PORB (Table 1). The misfit of the surface wave dispersion is defined as:

$$Q_v = \sqrt{\frac{\sum_{i=1}^{n}\left[5(V_i^o - V_i^c)^2/\sigma_i^2 - 4D_i^2/\sigma_i^2\right]}{\sum_{i=1}^{n}\left[1/\sigma_i^2\right]}} \quad (1)$$

where n is the number of observations; V_i^o and V_i^c are the observed and calculated phase velocities for ith data point; σ_i is the assigned observation error of V_i^o; D_i is the smaller of $|V_i^o - V_i^c|$ and σ_i. In Eq. (1), data points more than one σ_i from the calculated dispersion curve will contribute to the misfit functions with a larger weight compared with the normal squared residual. If the residual of all points are lower than σ, the misfit function reduces to the usual rms residual. This choice of misfit function penalizes models with large residuals and helps to force the solutions to stay within the observed error bounds.

Besides the phase velocities, we included the average $(Ps-P)_o$ time, measured with the receiver functions, as additional constraint. For simplicity, we call $(Ps-P)_o=t$, with observed and calculated values being t_o and t_c, respectively. The observed average value of PAZB and PORB is: $t_o \pm \sigma_t = 4.1 \pm 0.2$ s (Table 1). We define the misfit of the Ps times as $Q_t = 2|t_o - t_c| - D_t$, where D_t is the smaller of $|t_o - t_c|$ and σ_t.

We combined the two objectives (fitting phase velocities and Ps times) in a sum of weighted

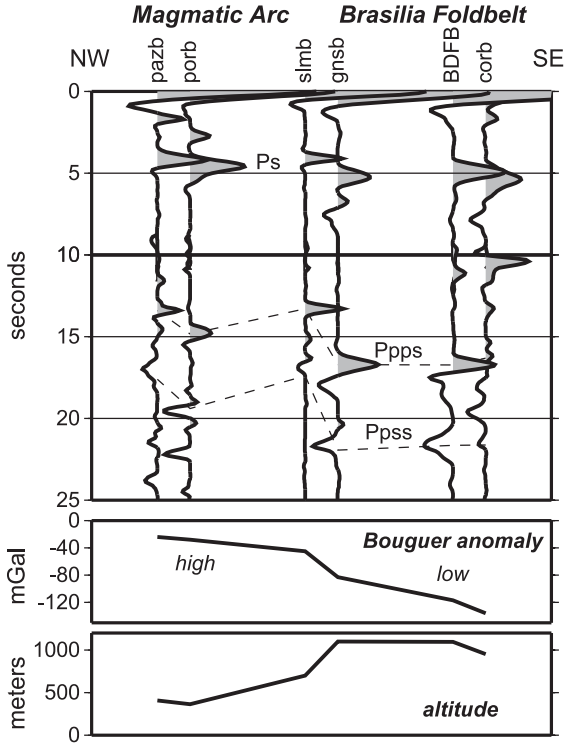

Fig. 6. NW–SE pseudo cross-section of stacked receiver functions (top) for a reference slowness of 8.0 s/°. Receiver functions were slant stacked in two different windows, with different slopes, to enhance the Moho converted Ps phase (shown from 0 to 10 s) and to enhance the multiply reflected Ppps phase (from 10 to 25 s). The top dashed line indicates the observed positive Ppps peak; the lower dashed line indicates the expected time of the negative Ppss peak. Bouguer anomalies (middle) and altitudes (bottom) for each station: higher gravity and lower altitudes for the thinner crust of the Magmatic Arc suggest isostasy is achieved mainly by Moho topography (Airy type compensation).

objective functions, Q (Eq. (2)), where w is the weight:

$$Q = Q_v + wQ_t \quad (2)$$

We carried out GA inversions for models with five layers: sediments, upper crust, lower crust, lithospheric lid and asthenosphere, and searched for both thickness and V_s. The search ranges, discretized with 12 bits, are shown in Table 3. Four different weights (0.0–0.017) were used. For each weight, Q was optimized for more than 15 runs, and all good models were saved. We used a population of 25 models and 500 generations, with a cross-over rate of 0.85 and mutation rate of 0.02.

Fig. 8 shows all the best models (misfit of the phase velocities Q_v<0.015 km/s), and the corresponding fit to the observed dispersion data. The general trend of the S-velocity can be observed with values around 4.0 km/s in the lower crust. If we further select the models with Ps misfit Q_t<0.1 s, the variability of the models is considerably reduced (Fig. 8c) and the crustal thickness shows up at about 35 km, in good agreement with the receiver function results for PAZB and PORB (Table 1). Fig. 9 compares the average S-wave profiles (average and one standard deviation obtained from all models in Fig. 8c) with the P-wave profile beneath station PORB obtained from the deep refraction line (Berrocal et al., 2004). The surface wave profile shows relatively lower velocities in the first 3 km, but the available period range of the surface waves (>10 s) does not allow enough resolution at such shallow depths. At mid crustal depths, S velocities are relatively higher, compared with those expected from the seismic line near PORB. This could be an indication of varying Vp/Vs ratios with depth (from ~1.8 in the upper crust to ~1.7 in the lower crust). Alternatively, it could also mean that the average S-wave velocity for the whole Magmatic Arc is higher than the small section sampled by the seismic line. Detailed comparison of the two profiles is not justified because they do not sample exactly the same crustal segments. The two profiles, however, give a very consistent average crustal depth of 35–36 km for the Magmatic Arc.

An interesting feature of the surface wave models is a rather low S-wave velocity for the topmost upper mantle (V_s ~4.4 km/s, Figs. 8c and 9). The upper mantle P-wave velocities (obtained for the seismic refraction line) are lower beneath the Magmatic Arc (about 8.0 km/s) and higher beneath the Brasília foldbelt (about 8.25 km/s). Our results indicate that the Vp/Vs ratio in the upper mantle beneath the Magmatic Arc is about 1.80, a value consistent with the commonly used ratio of 1.78 for the upper mantle. The increase in S velocities deeper in the upper mantle (Fig. 8c) is not well constrained by our surface wave data because we did not have periods longer than about 65 s. The generally low S-wave velocity in the lithosphere is also consistent with the low-velocity P-wave anomaly beneath the Magmatic Arc (about −1%) obtained in the teleseismic

Table 2
Earthquakes used for the PAZB-PORB interstation phase velocities

Year	Day	Time	Lat. (°)	Long. (°)	Depth (km)	m_b	M_S	Dist. (°)	BAz (°)
2000	267	02:17:44.1	4.287	−32.636	10	5.5	5.5	23.9	44.1
2001	205	17:42:41.3	−32.854	−71.366	33	5.6	4.7	28.1	222.6
2001	283	10:02:00.3	5.729	−32.749	10	4.7	4.7	24.9	41.6
2001	288	15:19:49.4	−33.126	−72.187	23	4.9	4.7	28.8	223.0

tomography, compared with the foreland domain, as shown below.

4. Upper mantle tomography

Travel time residuals of teleseismic P and PKP phases were inverted in a tomographic study of the upper mantle in southeastern and central Brazil (Assumpção et al., 2004; Rocha and Assumpção, 2003; Schimmel et al., 2003). Relative residuals were determined by waveform cross-correlation. In addition to P-wave anomalies, defined in a grid with spacing of about 0.33°, the inversion included station corrections and small (heavily damped) epicentral mislocation. Smoothness constraints (minimizing both first and second model derivatives) were used to regularize the inversion. Residuals larger than 1.5 standard deviations were downweighted to reduce effects of possible outliers. Schimmel et al. (2003) give more details of the data processing and inversion methods.

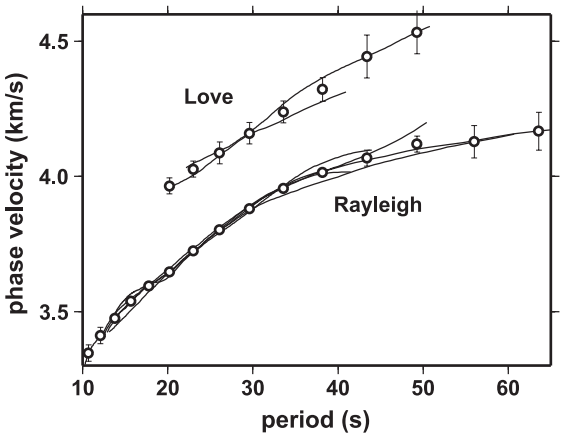

Fig. 7. Observed phase velocities between PAZB and PORB for the four events of Table 2. Circles are average velocities with standard errors used in the GA inversion. For the event 2001/205, both vertical and radial components of the Rayleigh wave were used.

Rocha and Assumpção (2003) and Assumpção et al. (2004) inverted data for all southeastern and central Brazil consisting of more than 10,000 P-wave readings at more than 50 stations, twice the amount of data used by Schimmel et al. (2003). The relative residuals ranged roughly from −1 to +1 s (rms of 0.41 s). After the inversion, the tomographic model explained about 88% of the data, with final residuals having rms deviations of about 0.05 s. Fig. 10 shows the anomaly map of central Brazil, where nine stations of the total set are located, with lower P-wave velocities in the west (dark gray) and higher velocities in the east (light gray). Because of the large station separation, the geometry of the ray paths does not allow sufficient vertical resolution in the top 200 km. For this reason, the anomalies shown in Fig. 10 are average values from the Moho to the bottom of the lithosphere. Clearly, the small number of stations in Central Brazil does not allow a detailed imaging of the upper mantle. However, several inversion tests were carried out by removing one station at a time, and the regional pattern of low velocities in the west and high in the east was a robust feature.

It is interesting to notice that the upper mantle beneath the Magmatic Arc and the Goiás Massif has lower P-wave velocities compared with the internal and external zones of the Brasília belt foreland domain. This is in good agreement with the results

Table 3
Search ranges for the GA inversion of phase velocities

Layer	Thickness (km)	S velocity (km/s)
Sedimentary	1–4	2.4–3.2
Upper crust	5–30	3.0–4.0
Lower crust	5–30	3.5–4.5
Lithospheric lid	30–50	4.0–5.2
Asthenosphere	halfspace	4.0–5.2

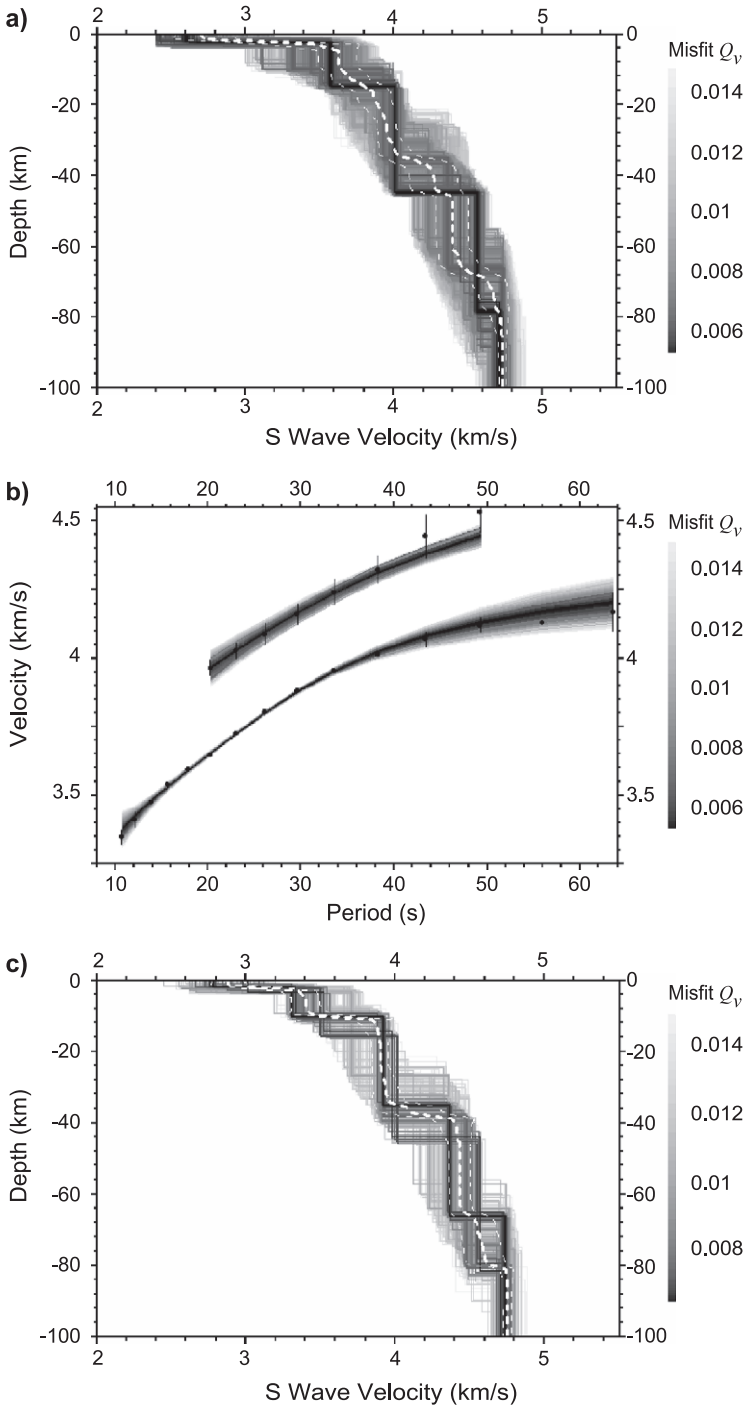

Fig. 8. Inversion of the phase velocities. (a) All best models (phase velocity misfit Q_v<0.015 km/s) after 15 runs of the GA algorithm allowing S-velocity and thickness to vary. (b) Calculated dispersion curves for all best models shown in (a). (c) Selection of the best models that also fit the Ps times to within 0.1 s (misfit Q_t<0.1 s). Notice the sharper definition of the Moho discontinuity. White dashed lines are the misfit-weighted averages with one standard deviation.

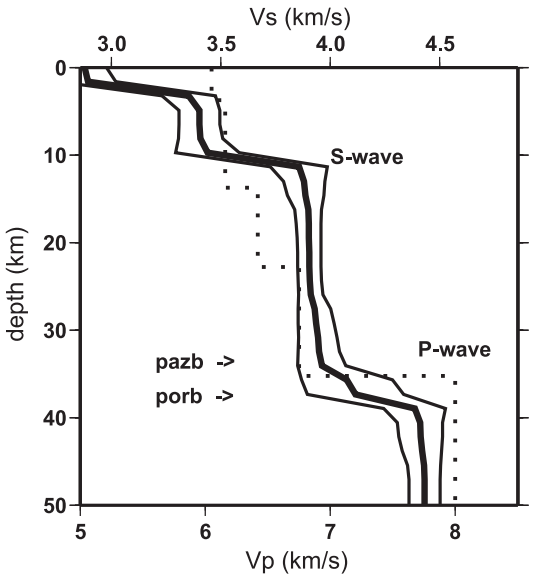

Fig. 9. Comparison of the S-wave profile along the path PAZB-PORB from surface-wave inversion (solid lines) with the P-wave profile ("staircase" dotted line) beneath station PORB on the seismic refraction line. The S-wave lines are the average profile (thicker line) with one standard deviation (thin lines) taken from Fig. 8c. The two arrows indicate the Moho depths from the receiver functions at stations PAZB and PORB (Table 1). The Vp scale (bottom) and the Vs scale (top) obey the ratio Vp/Vs=1.75.

of the seismic refraction line (Berrocal et al., 2004) where Pn velocity is 8.0 km/s beneath the Magmatic Arc and 8.20–8.25 km/s beneath the external zone (Fig. 10). The amplitudes of the tomography anomalies seem small (about ±0.5%), but they are actually lower bounds because of the strong smoothness constraints necessary to regularize the inversion. For this reason, the values of the tomography anomalies are not inconsistent with the difference in the Pn velocities measured in the seismic refraction line (±1.5%).

5. Discussion and conclusions

Crustal and upper mantle properties in the northern part of the Tocantins Province follow the same SSW–NNE trend and correlate with the main geological units. The upper mantle has relatively low P and S velocities beneath the Magmatic Arc and the Goiás Massif. The Magmatic Arc has thinner crust, with average Vp/Vs ratios varying from 1.74 to 1.76 probably indicating predominantly mafic granulitic rocks in the lower crust. This is consistent with strong uplift at the end of the Neoproterozoic accompanied by mafic intrusions in the crust (possibly underplating) causing intense granitic/gabbroic magmatism, a characteristic feature of the Magmatic Arc (Pimentel et al., 1996; Laux et al., 2003).

The foreland domain of the Brasília foldbelt has thicker crust, determined both by the seismic refraction line and the receiver functions. The crustal average Vp/Vs ratio is low (about 1.70) suggesting predominantly felsic granulites in the lower crust of the external zone adjacent to the São Francisco craton. Teleseismic tomography shows relatively high P-wave velocities in the upper mantle, consistent with the high Pn velocities observed in the seismic refraction line (8.20–8.25 km/s). No signifi-

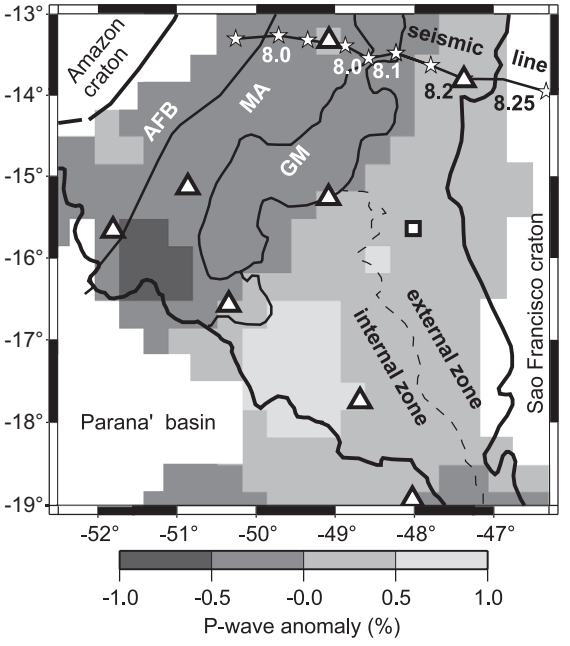

Fig. 10. Lateral variation of P-wave velocity (in percentage) at 150 km depth determined with teleseismic tomography. Geological units labelled as in Fig. 1b. Note high velocities beneath the foreland domain of the Brasília foldbelt (light gray areas) compared with lower velocities beneath the Magmatic Arc and Goiás Massif (dark areas). Numbers next to the seismic refraction line are Pn velocities showing similar pattern to the tomography anomalies. Triangles and square are the nine stations in this area used in the regional tomography of SE Brazil (Schimmel et al., 2003; Rocha and Assumpção, 2003). White areas have less than 15 rays/cell at depth and are outside the resolution limit.

cant contrast in the upper mantle was observed across the foldbelt/craton surface limit shown in Fig. 10.

The western limit of the São Francisco craton has been a matter of dispute (Alkmin et al., 1993). Figs. 1b and 10 show the most commonly accepted western limit (Almeida, 1981) based on large thrust faults over Bambui sediments. Almeida (1981), however, had noted that this limit is transitional and in many places a matter of convention. The seismic refraction line (Berrocal et al., 2004) does not show any significant discontinuity in crustal properties near the limit shown in Fig. 10, except for a general westward dip of all crustal layers and a thickening of the superficial metasedimentary layer.

Compilations of crustal P- and S-wave velocity profiles worldwide indicate that the lower crust of Archean cratons are most often characterized by relatively more felsic rocks compared with Proterozoic crust (e.g., Durrheim and Mooney, 1991). Assumpção et al. (2002) showed that the Archean block in the southern part of the São Francisco craton also has low Vp/Vs ratio (about 1.70–1.71). The low Vp/Vs ratios in the Brasília foreland domain, together with high velocities in the upper mantle, are consistent with the hypothesis that the lithospheric boundary of the São Francisco craton extends further to the west beneath the foreland domain of the Brasília foldbelt.

Alkmin et al. (1993) proposed that the surface limit of the São Franciso craton was only the stable foreland block of a larger "San Franciscan plate", which included all of the foreland domain of the Brasilia foldbelt. Alkmin et al. (2001) included the Goiás Massif as part of the Neoproterozoic São Francisco-Congo continental block. Pimentel et al. (2000), on the other hand, place the limit of the São Francisco-Congo continental plate just east of the Goiás Massif. Although the number of stations of our study is rather limited, our integrated results show the highest contrast between crustal and upper mantle properties (including the Bouguer anomalies) between the Goiás Massif and the Brasília belt external zone. Our data seem to favour the Neoproterozoic suture marking the final collision between the São Francisco-Congo and the Amazon plates at the boundary between the Goiás Massif and the foreland domain of the Brasília foldbelt.

Acknowledgments

Project supported by FAPESP grants 96/01566-0, 00/07134-2, CNPq grants 30.0227/79-5, 52.0078/00-4 and CT-Mineral Fund. We thank Bob Herrmann (St. Louis University) for discussions on surface wave processing, Martin Schimmel (CSIC, Barcelona) for help in the tomography work, and Márcio Pimentel and Reinhardt Fuck (Univ. of Brasília) for discussions on the geology. We also thank Anya Reading and Frank Graeber for detailed comments on a preliminary version of the paper.

References

Abers, G.A., 1998. Array measurements of phases used in receiver-function calculations: importance of scattering. Bull. Seismol. Soc. Am. 88, 313–318.

Alkmin, F.F., Neves, B.B.B., Alves, J.A.C., 1993. Arcabouço tectônico do cráton do São Francisco-uma revisão. In: Domingues, J., Misi, A. (Eds.), O Cráton do São Francisco. Soc. Bras. Geologia, Brazil, pp. 45–62.

Alkmin, F.F., Marshak, S., Fonseca, M.A., 2001. Assembling West Gondwana in the Neoproterozoic: clues from the São Francisco craton region, Brazil. Geology 29, 319–322.

Almeida, F.F.M., 1981. O cráton do Paramirim e suas relações com o do São Francisco. Proc. Symp. "Cráton do São Francisco e suas faixas marginais". Soc. Bras. Geologia, Salvador, Brazil, pp. 1–10.

Ammon, C.J., Randall, G.E., Zandt, G., 1990. On the nonuniqueness of receiver function inversions. J. Geophys. Res. 95, 15303–15318.

Assumpção, M., James, D., Snoke, J.A., 2002. Crustal thicknesses in SE Brazilian shield by receiver function: implications for isostatic compensation. J. Geophys. Res. 107 (B1), 2006 (pp. ESE2-1-14).

Assumpção, M., Schimmel, M., Escalante, C., Barbosa, J.R., Barros, L.V., 2004. Intraplate seismicity in SE Brazil: stress concentration in lithospheric thin spots. Geophys. J. Int. 158 (in press).

Berrocal, J., Marangoni, Y., Sá, N.C., Fuck, R., Soares, J.E.P., Perosi, F., Fernandes, C., 2004. Deep seismic refraction and gravity crustal model and tectonic deformation in Tocantins Province, central Brazil. Tectonophysics 388, 187–199 (this volume).

Christensen, N.I., 1996. Poisson's ratio and crustal seismology. J. Geophys. Res. 101, 3139–3156.

Durrheim, R.J., Mooney, W.D., 1991. Archean and Proterozoic crustal evolution: evidence from crustal seismology. Geology 19, 606–609.

França, G.S.L., Assumpção, M., 2004. Crustal structure of the Ribeira fold belt, SE Brazil, derived from receiver functions. J. South Am. Earth Sci. 16, 743–758.

Herrin, E., Goforth, T., 1977. Phase-matched filters: application to the study of Rayleigh waves. Bull. Seismol. Soc. Am. 67, 1259–1275.

Herrmann, R.B., 1973. Some aspects of band-pass filtering of surface waves. Bull. Seismol. Soc. Am. 63, 663–671.

Herrmann, R.B., 1987. Computer programs in Seismology. St. Louis University, St. Louis, MO.

Holbrook, W.S., Mooney, W.D., Christensen, N., 1992. The seismic velocity structure of the deep continental crust. In: Fountain, D.M., Arculus, R., Kay, K.W. (Eds.), Continental Lower Crust, Develop. in Geotectonics, vol. 23. Elsevier, New York, pp. 1–34.

Junges, S.L., Pimentel, M.M., Moraes, R., 2002. Nd isotopic study of the Neoproterozoic Mara Rosa Arc, central Brazil: implications for the evolution of the Brasília Belt. Precambrian Res. 117, 101–118.

Laux, J.H., Pimentel, M.M., Dantas, E.L., Armstrong, R., Armele, A., 2003. Basic magmatism associated with the Goiás magmatic arc in Anicuns, GO, central Brazil: new ID-TIMS and SHRIMP U–Pb data. Proc. IV South American Symp Isotope Geology, Salvador, Brazil. CD-ROM.

Marangoni, Y., Assumpção, M., Fernandes, E.P., 1995. Gravimetria em Goiás. Rev. Bras. Geofís. 13, 205–219.

Owens, T.J., Zandt, G., Taylor, S.R., 1984. Seismic evidence for an ancient rift beneath the Cumberland plateau, Tennessee: a detailed analysis of broadband teleseismic P waveforms. J. Geophys. Res. 89, 7783–7795.

Pimentel, M.M., Fuck, R.A., 1992. Neoproterozoic crustal accretion in central Brazil. Geology 20, 375–379.

Pimentel, M.M., Heaman, L., Fuck, R.A., 1991. Zircon and sphene U–Pb geochronology of upper Proterozoic volcanic-arc rock units from SW Goiás, central Brazil. J. South Am. Earth Sci. 4, 295–305.

Pimentel, M.M., Fuck, R.A., Alvarenga, C.J.S., 1996. Post-Brasiliano (Pan-African) high-K granitic magmatism in central Brazil: the role of late Precambrian/early Paleozoic extension. Precambrian Res. 80, 217–238.

Pimentel, M.M., Whitehouse, M.J., Vianna, M.D., Fuck, R.A., Machado, N., 1997. The Mara Rosa arc in the Tocantins province: further evidence for Neoproterozoic crustal accretion in central Brazil. Precambrian Res. 81, 299–310.

Pimentel, M.M., Fuck, R.A., Botelho, N.F., 1999. Granites and the geodynamic history of the Neoproterozoic Brasília belt, central Brazil: a review. Lithos 46, 463–483.

Pimentel, M.M., Fuck, R.A., Jost, H., Ferreira Filho, C.F., Araújo, S.M., 2000. The basement of the Brasília Fold Belt and the Goiás Magmatic Arc. In: Cordani, U.G., Milani, E.J., Thomaz Filho, A., Campos, D.A. (Eds.), The Tectonic Evolution of South America, Rio de Janeiro, 31st. Intern. Geol. Congress, DNPM, Brasilia, Brazil, pp. 195–229.

Piuzana, D., Pimentel, M.M., Fuck, R.A., Armstrong, R., 2003. Neoproterozoic granulite facies metamorphism and coeval granitic magmatism in the Brasília Belt, central Brazil: regional implications of new SHRIMP U–Pb and Sm–Nd data. Precambrian Res. 125, 245–273.

Rocha, M.P., Assumpção, M., 2003. Tomografia sísmica do manto superior no Sudeste e centro-oeste do Brasil. Proc. VIII Int. Congr Braz. Geophys. Soc., Rio de Janeiro. CD-ROM.

Sá, N.C., Ussami, N., Molina, E.C., 1993. Gravity map of Brazil I: representation of free-air and Bouguer anomalies. J. Geophys. Res. 98, 2187–2197.

Schimmel, M., Paulssen, H., 1997. Noise reduction and detection of weak, coherent signals through phase-weighted stacks. Geophys. J. Int. 130, 497–505.

Schimmel, M., Assumpção, M., VanDecar, J.C., 2003. Seismic velocity anomalies beneath SE Brazil from P and S wave travel time inversions. J. Geophys. Res. 108 (B4), 2191 (ESE 3-1-5).

Zandt, G., Ammon, C.J., 1995. Continental crust composition constrained by measurements of crustal Poisson's ratio. Nature 374 (6518), 152–154.

Zandt, G., Myers, S.C., Wallace, T.C., 1995. Crust and mantle structure across the Basin and Range-Colorado Plateau boundary at 37° latitude and implications for Cenozoic extensional mechanism. J. Geophys. Res. 100 (B6), 10529–10548.

Zhu, L., Kanamori, H., 2000. Moho depth variation in southern California from teleseismic receiver functions. J. Geophys. Res. 105 (B2), 2969–2980.